Proton NMR Relaxation Study of the Dynamics of Anthopleurin-A in Solution

ANDREW E. TORDA and RAYMOND S. NORTON,* *School of Biochemistry, University of New South Wales, Kensington, 2033, Australia*

Synopsis

Spin–spin and spin–lattice ^{1}H-nmr relaxation times of the sea anemone polypeptide anthopleurin-A were measured at frequencies of 200, 300, 400, and 500 MHz. Relaxation times were fitted iteratively by least squares regression to the isotropic tumbling model, Woessner's model for anisotropic motion, and Lipari and Szabo's "model-independent" model. Data for aromatic and aliphatic methine protons could not be fitted satisfactority using the isotropic model. Good fits were obtained, however, using the model-independent approach, indicating that high-frequency internal motions of the polypeptide backbone were significant. In addition, a range of τ_c values from 2.2 to 3.2 ns was obtained for various methine protons, suggesting that overall rotational reorientation of the molecule was anisotropic. Methyl group relaxation data were fitted satisfactorily by Woessner's model. Some assessment has been made of the effect of experimental errors on the quality of fit to the data, as well as of the contribution of experimental values at certain frequencies to definition of the spectral density function.

INTRODUCTION

Anthopleurin-A (AP-A) is a polypeptide of 49 residues containing three disulfide bonds and having a M_r of 5138. It is extracted from the northern Pacific sea anemone *Anthopleura xanthogrammica* and is a member of an homologous series of polypeptides spanning several species.[1] AP-A is of pharmacological interest because of its potent positive inotropic activity on the mammalian heart. In this respect it resembles the clinically used cardiac glycosides, but AP-A has a higher therapeutic index and fewer side effects, and acts by a different mechanism.[2] Although its antigenicity has prevented its direct clinical use, an understanding of its solution structure and dynamics, combined with a knowledge of regions essential for activity, should provide an understanding of the molecular basis of its activity, which may ultimately allow it to serve as a starting point for the design of smaller, nonantigenic analogues.

AP-A has been crystallized,[3] although no structure has yet been published. The molecule's solution properties have, however, been studied extensively by nmr spectroscopy. The 300-MHz spectrum has been largely assigned,[4] specific regions of secondary structure identified,[5] and most recently, a low-resolution structure determined.[6] The rates at which many of the backbone amide protons exchange with the solvent have also been determined and are consistent with the proposed secondary structure.[7] The aim of the present work is

*To whom correspondence should be addressed.

Biopolymers, Vol. 28, 703–716 (1989)

CCC 0006-3525/89/030703-14$04.00

to use proton relaxation measurements at frequencies from 200 to 500 MHz to characterize the dynamics of this polypeptide in solution, and in the course of the analysis, to assess the errors generally present in this type of measurement.

^{13}C-nmr spin–lattice relaxation time (T_1) and nuclear Overhauser enhancement (NOE) measurements have often been used to obtain correlation times for overall tumbling of proteins[8] and some internal motions.[9-13] The ^{13}C nucleus has the advantages that relaxation can be assumed to be dipolar due to bonded protons and the geometry of the relaxation system of the proton-bearing carbons is well characterized. ^{1}H-nmr relaxation measurements have been used less often for a number of reasons, including their greater susceptibility to spin diffusion,[14-16] the presence of cross-correlation between internuclear vectors with the same motions,[17,18] poorer resolution in one-dimensional spectra, and that nonbonded neighbors may contribute to the relaxation. The proton's greater sensitivity for nmr detection, however, can be valuable when signal to noise is limiting due to a low protein concentration or other factors.

Measurement of several different ^{1}H-nmr relaxation parameters is experimentally possible, although each can be expressed in terms of an internuclear distance and a linear combination of samplings of the spectral density function describing the motions of the specific internuclear vector. Selective T_1 and selective NOE measurements[19-21] have been used to obtain correlation times and estimate internuclear distances in peptides. Selective NOEs and their buildup rates have been used to examine internal motions in the protein lysozyme, where internal distances are known from x-ray crystallography.[22] A combination of T_1 and T_2 measurements has been used to obtain both overall and internal motional correlation times in the polypeptide erabutoxin.[23]

In the case of AP-A, only a low-resolution structure based on nmr data is currently available,[6] which is not sufficiently precise to permit accurate estimates to be made of the distances from a proton of interest to its immediate neighbors. Thus, the internuclear distances and number of relevant interactions had to be treated as variables. We therefore chose to use a series of T_1 and T_2 measurements spanning as large a range of frequencies as was practically possible and to simultaneously combine all the data for analysis. This strategy allowed the sampling of motions at a large range of frequencies before attempting to fit them to specific models describing internal motions.

MATERIALS AND METHODS

Experimental

AP-A was isolated from *A. xanthogrammica* by the method of Schweitz et al.[24] Protein was used for nmr after desalting on Sephadex G-10 or by reverse-phase high performance liquid chromotography. D_2O ($\geq$ 99.75% D) was obtained from the Australian Atomic Energy Commission (Lucas Heights, New South Wales, Australia) and NaOD and DCl from Merck, Sharpe and Dohme (Montreal, Canada). pH values of samples were measured at 22°C with an Activon Model 101 pH meter and Ingold microelectrode. Reported values are meter readings, uncorrected for deuterium isotope effects.

Exchangeable sites were fully deuterated by twice lyophilising from D_2O after incubating at room temperature for > 48 h. Samples were prepared by dissolving protein in D_2O containing 0.1 mM EDTA, and adjusting the pH to between 4.8 and 5.3, a range over which no significant changes occurred in the spectrum.[25] The sample was bubbled with and sealed under analytical grade nitrogen. One sample was used for measurements at 200, 300, and 400 MHz. Although a fresh sample was used at 500 MHz, reproducibility of results was checked by repeating the 300-MHz measurements with the new sample. Solutions were 4.8 mM in AP-A.

Spectra were recorded at 300 K at 200, 300, 400, and 500 MHz on Varian XL-200, Bruker CXP-300, Jeol GX-400, and Bruker AM-500 spectrometers, respectively, with quadrature detection and 8192 time domain points, except at 500 MHz where 16,384 time domain points were used. Spin–lattice relaxation measurements were made using the inversion-recovery method,[26]

$$\text{delay} - 180° - \tau - 90° - \text{acquire}$$

with delay times of 6, 6, 8, and 9 s, at frequencies of 200, 300, 400, and 500 MHz, respectively. Although the 180° pulse width was adjusted before each series of measurements and was short enough to ensure complete inversion over the spectral width, its imperfections were accounted for in the data analysis (see below). Spin–spin relaxation rates were measured with the Meiboom–Gill modification of the Carr–Purcell method,[27]

$$\text{delay} - 90^\circ_x - \left(\tau - 180^\circ_y - \tau\right)_n - \text{acquire}$$

where the delays were the same as in the spin–lattice relaxation measurements. The period 2τ was 2 ms, short enough to avoid J modulation,[28] and even numbers of echoes were recorded. The sample was not spun and at least one spectrum was recorded with a large number of echoes to ensure that there was no steady state magnetization arising from field inhomogeneity.[29]

Data Analysis

To follow the behavior of resonances during relaxation measurements, peak heights were measured for well-resolved resonances in the proton spectrum. This resulted in data being obtained for three aromatic protons, two α-protons and three methyl groups. Some results are missing from Table I due to poorer resolution at the lowest frequency.

Ideally, the recovery rate of a proton in an inversion-recovery experiment is given by

$$M_t = M_\infty\left(1 - Ae^{-\frac{t}{T_1}}\right) \tag{1}$$

where M_t is the magnetization at a given t, M_∞ is the magnetization in a fully relaxed spectrum, T_1 is the spin–lattice relaxation time, and the coefficient A reflects the degree of inversion, being 2 for a perfect π pulse. For fitting the data by least squares analysis,[30] the modification of Ejchart et al.[31] was

TABLE I
Relaxation Times of Aromatic and Aliphatic Protons for AP-A in D_2O[a]

Proton	200 MHz		300 MHz		400 MHz[b]	500 MHz	
	T_1	T_2	T_1	T_2	T_2	T_1	T_2
Trp 33 H2	0.96	0.235	1.41	0.260	0.207	2.79	0.169
Tyr 25 H(3,5)(a)[c]	0.82	0.186	1.55	0.247	0.186	1.33	0.098
Tyr 25 H(3,5)(b)	0.86	0.171	1.51	0.226	0.180	1.36	0.124
Trp 23 H2	—[d]	—	1.21	0.136	0.114	2.28	0.098
Cys 47 H^{α}(a)	0.74	—	1.47	0.124	0.078	2.96	0.090
Cys 47 H^{α}(b)	0.82	—	1.35	—	0.053	2.40	0.087
Cys 46 H^{α}(a)	0.61	0.123	1.17	0.129	0.126	1.72	0.054
Cys 46 H^{α}(b)	0.57	—	0.97	0.092	0.097	1.84	0.053
Thr 42 H^{γ}	0.31	0.079	0.47	0.148	0.104	0.43	0.078
Thr 17 H^{γ}	0.32	0.068	0.45	0.154	0.107	0.59	0.022
Thr 21 H^{γ}	0.27	0.059	0.28	0.049	0.062	0.36	0.032

[a]All times in seconds. Reproducibility (measured at 300 MHz) was within 10% for T_1 values and within 15% for T_2 values.
[b]T_1 results at 400 MHz were not used due to temperature instability during the measurements.
[c](a) and (b) refer to individual components of multiplets whose rates were analyzed separately.
[d]Data not obtained due to poorer resolution at the lowest frequency.

examined, where the coefficient A is replaced by $(1 - \cos\alpha)$ to give

$$M_t = M_\infty\left(1 - (1 - \cos\alpha)e^{-\frac{t}{T_1}}\right) \tag{2}$$

α being the flip angle of the inversion pulse. We found that this modification gave no change in the convergence of the fitting program. The measurements could also deviate from pure exponential behavior because of cross relaxation,[14-16] cross correlation,[17,18] or in the case of Thr 42, slight overlap with the highly split Leu 22 γ-methine multiplet. To account for this possibility, Eq. (2) was modified to include a second exponential independently weighted by a coefficient $(1 - \cos\beta)$. Although this gave five variable parameters, the fitting process was performed so as to favor one decay rate by setting the initial estimate of α to 180° and β to 0°. The initial step size for β was set to a fraction of a degree so as to encourage the program to converge with the smallest necessary contribution from the second decay. Typically, convergence was achieved with β between 0° and 5°, effectively a single exponential, but the largest contribution from a second decay was found for the methyl protons of Thr 42 at 300 MHz. In this case, the second decay accounted for 20% of the magnetization.

The decay rates of protons in T_2 measurements were usually fitted to

$$M_t = M_o e^{-\frac{t}{T_2}} \tag{3}$$

where M_o is the initial magnetization. Some of the methyl peaks showed slight nonexponential behavior which was attributed to cross-correlation between internuclear vectors with similar motions[23] and slight peak overlap. For these peaks, points were fitted to a biexponential decay, but experimental

data had been collected mostly at small numbers of echoes (< 100) to emphasize the initial decay and the fitting was again performed to favor a single decay rate. The most significantly biphasic behavior was shown by the methyl protons of Thr 42, where the second decay rate accounted for 25% of the total magnetization.

RESULTS AND DISCUSSION

Motional Models

Figure 1 shows regions of the 500-MHz spectrum of AP-A containing the well-resolved resonances used for analysis. The measured T_1 and T_2 values for these resonances are summarized in Table I. We have assumed that relaxation is predominantly dipolar, so that the results are related to the motional spectral density function by

$$\frac{1}{T_1} = \tfrac{3}{10}\gamma^4\hbar^2 \sum_{j\neq i} \left(r_{ij}^{-6}\right)\{J(\omega) + 4J(2\omega)\} \tag{4}$$

$$\frac{1}{T_2} = \tfrac{3}{20}\gamma^4\hbar^2 \sum_{j\neq i} \left(r_{ij}^{-6}\right)\{3J(0) + 5J(\omega) + 2J(2\omega)\} \tag{5}$$

where γ is the gyromagnetic ratio, r_{ij} the internuclear distance between i and j, and $J(\omega)$ the spectral density function which defines the specific model for the motions causing the relaxation. We have considered three different possibilities, chosen for their simplicity, physical applicability or generality.

If isotropic tumbling with a correlation time τ_c is the only important motion, the spectral density function is given by

$$J(\omega) = \frac{\tau_c}{1 + \omega^2\tau_c^2} \tag{6}$$

If an additional motion due to methyl group rotation is present, Woessner's model[32] is most appropriate. Given the known geometry of the interacting protons, $J(\omega)$ is given by

$$J(\omega) = \frac{1}{4} \cdot \frac{\tau_c}{1 + \omega^2\tau_c^2} + \frac{3}{4} \cdot \frac{\tau_{cl}}{1 + \omega^2\tau_{cl}^2} \tag{7}$$

where $1/\tau_{cl} = (1/\tau_c) + (1/\tau_{Me})$ for a three-sites jump model and τ_{Me} is the correlation time for methyl rotation. Where motion is not isotropic, but there is no reason to favor any specific physical model, the "model-free" approach of Lipari and Szabo[33] can be applied, in which

$$J(\omega) = \frac{2}{5} \cdot \left(\frac{\delta^2\tau_c}{1 + \tau_c^2\omega^2} + \frac{(1 - \delta^2)\tau}{1 + \tau^2\omega^2} \right) \tag{8}$$

where $1/\tau = (1/\tau_c) + (1/\tau_e)$, δ is the generalized order parameter and τ_e is the effective correlation time for internal motions.

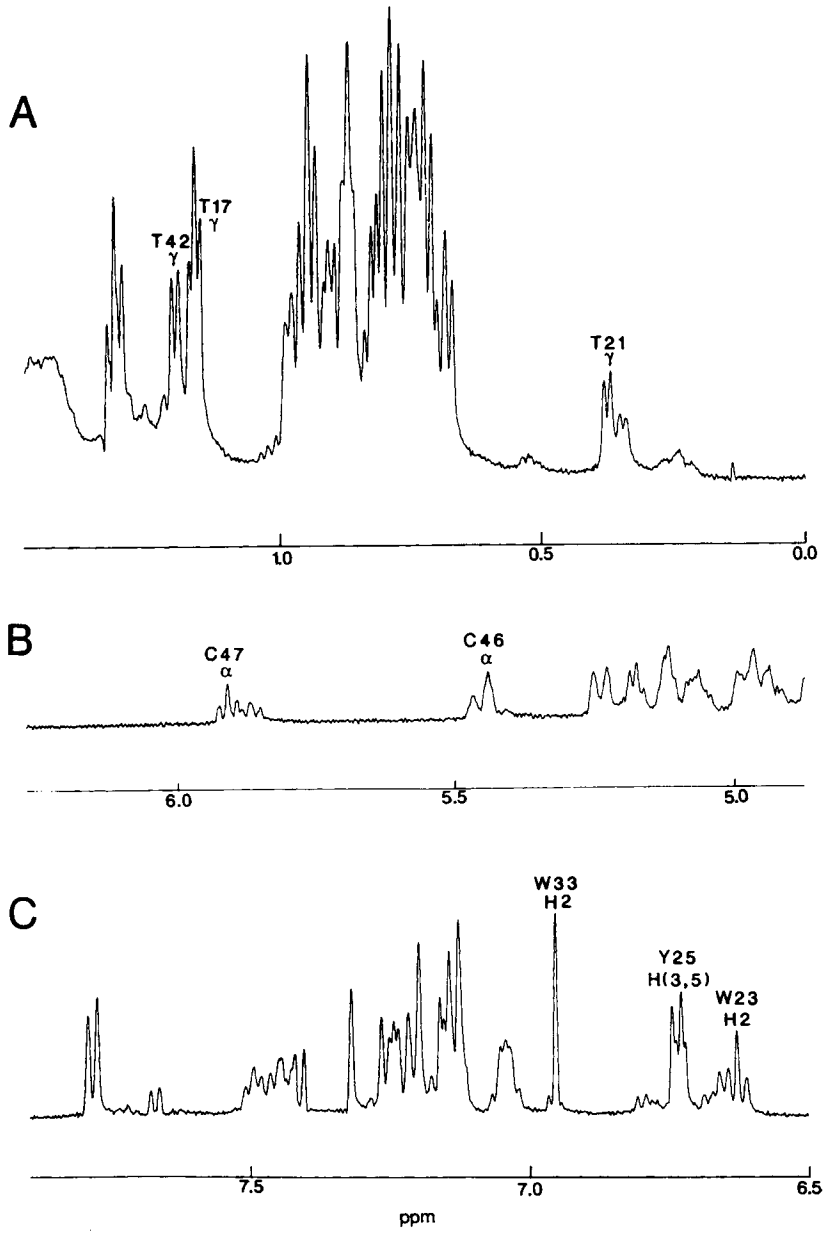

Fig. 1. Regions of methyl (A), downfield α-proton (B), and aromatic (C) resonances of 500-MHz ^{1}H-nmr spectrum of AP-A in D_2O. Peaks marked are those whose relaxation times were analyzed (cf. Table I).

In the case of isotropic motion, the T_1/T_2 ratio could be used to calculate τ_c at each frequency. Similarly, for models with more than one variable parameter, one could attempt to manually calculate values that explained the measurements. We have instead used an iterative least squares fitting procedure to perform simultaneous regression onto Eqs. (4) and (5) substituted with the appropriate spectral density function from Eq. (6), (7), or (8). The

spectrometer frequency was treated as the independent variable, and measured T_1 and T_2 values as the dependent variables in the manner of Craik et al.[34] For the case of aromatic and aliphatic methine protons, relaxation will be caused by an unknown number of protons at unknown distances. Thus, when fitting the data to either isotropic motion or model-free models, the internuclear distance r must be treated as a variable parameter, as must a coefficient n to account for summation over all interacting protons. Because these two parameters simply affect the scaling of Eqs. (4) and (5), their effect is indistinguishable in these measurements, and it is only necessary to vary one while setting the other to some arbitrary value. In the case of Woessner's model applied to methyl groups, the distance r was taken to be 0.179 nm and the interaction summed for two protons. When fitting relaxation data to models including internal motions, it is common to use a value for the overall tumbling correlation time obtained from either rigid backbone proton relaxation data or some other physical technique such as light scattering. As will be shown below, this was not possible for AP-A. This resulted in two variable parameters when fitting to isotropic motion, two for Woessner's model and four for the Lipari and Szabo model. Given that seven measurements were available, the problem was in principle more than adequately defined (although see below). To test the aptness of each model, we used the correlation coefficient as a measure of fit. This criterion established quite clearly whether or not the data were reasonably explained.

Analysis of Proton Relaxation Rates

The spectrum of AP-A contained only two α-proton resonances that were sufficiently well resolved to be amenable to analysis at all frequencies, as shown in Fig. 1. As both were from disulfide-bonded cysteine residues, it appeared likely that they would be rigid with respect to the polypeptide backbone and would thus serve as points from which to obtain a correlation time for overall molecular tumbling. Similarly, as NOE measurements have shown that the aromatic rings of Trp 23 and 33 and Tyr 25 are close to many other residues in the molecule,[5] and therefore possibly motionally constrained, an attempt was also made to fit the relaxation behavior of their resonances to the isotropic motion model. Fitting of data for these and the two α-protons gave in all cases a correlation coefficient < 0.85. Thus, it was clear that this simple model was inadequate to describe the motions of any of these protons in AP-A.

Having no reason to favor any physical description of additional motions, we then chose to fit data using Eq. (8), as shown in Table II. From the correlation coefficients of the fits, this model does seem to adequately describe the measured relaxation times. Each of these protons displays one rapid motion ($\tau_e < 0.3$ ns) and one slower motion ($\tau_c > 2$ ns), corresponding to internal and overall motions, respectively. This is consistent with the poor fit found for the isotropic motion model. It is also apparent from Table II that the correlation time for overall motion varies from 2.2 to 3.2 ns. This suggests that, aside from the summed effects of internal and overall motions, there is also a detectable anisotropy in the overall tumbling of the molecule. This is perhaps not surprising considering the distinctly ellipsoidal shape of some

TABLE II
Aromatic and Aliphatic Methine Proton Relaxation Data Fitted to Order Parameter Model[33]

Proton	τ_c (ns)	τ_e (ns)	δ	r
Trp 33 H2	2.7	0.3	0.8	0.999
Tyr 25 H(3,5)	3.2	0.005	0.2	0.972
Trp 23 H2	2.2	0.04	0.8	0.999
Cys 47 H^{α}	2.5	0.04	0.7	0.991
Cys 46 H^{α}	2.7	0.2	0.9	0.997

TABLE III
Methyl Proton Relaxation Data Fitted to Woessner's Model[32]

Proton	τ_c (ns)	τ_{Me} (ns)	r
Thr 17 H^{γ}	2.6	0.043	0.990
Thr 21 H^{γ}	4.4	0.088	0.991
Thr 42 H^{γ}	2.5	0.051	0.980

other well-studied proteins. For example, the ratios of the major axes in lysozyme[35] and bovine serum albumin[36] are 2 and 3.5, respectively, leading to anisotropic overall motion.[8]

The relaxation behavior of the methyl protons was treated differently from those of the methine protons considered so far. In this particular case, the geometry of the protons bound to the methyl carbon is known, so the analysis is simplified. If a single correlation time for overall tumbling were applicable, fitting to Woessner's model [Eq. (7)] would be trivial, needing only to be solved for τ_{Me}. Instead, in the case of AP-A, it was necessary to treat τ_c as a variable during the fitting procedure. The results of a simple two-parameter fitting are shown in Table III. The worst correlation coefficient is 0.98 for the methyl group of Thr 42. Although any data fitting can be improved by introducing more variable parameters (here, for example, a third correlation time and weighting coefficient[37]), this is only justified when it will significantly improve the quality of the fit. Considering the presence of experimental error, we consider the data to be adequately explained and further motions to be undetectable.

Effects of Experimental Errors

Relatively few physical assumptions have been made in analyzing the data presented here. There is good evidence that all the observed sites experience a significant motional anisotropy, but there is no justification at this stage for choosing any one physical interpretation over another. Even in this simple analysis, it is worthwhile to consider the information content of each measurement and the uncertainty of the fitted parameters introduced by experimental error. The spectrum of a polypeptide such as AP-A is typically quite crowded, and the highest magnetic field strength is desirable for resolution of a useful number of resonances in one-dimensional nmr spectra (cf. Fig. 1). We have therefore examined the effect of experimental errors at 600 MHz, the highest frequency currently available with commercial spectrometers. Spin–

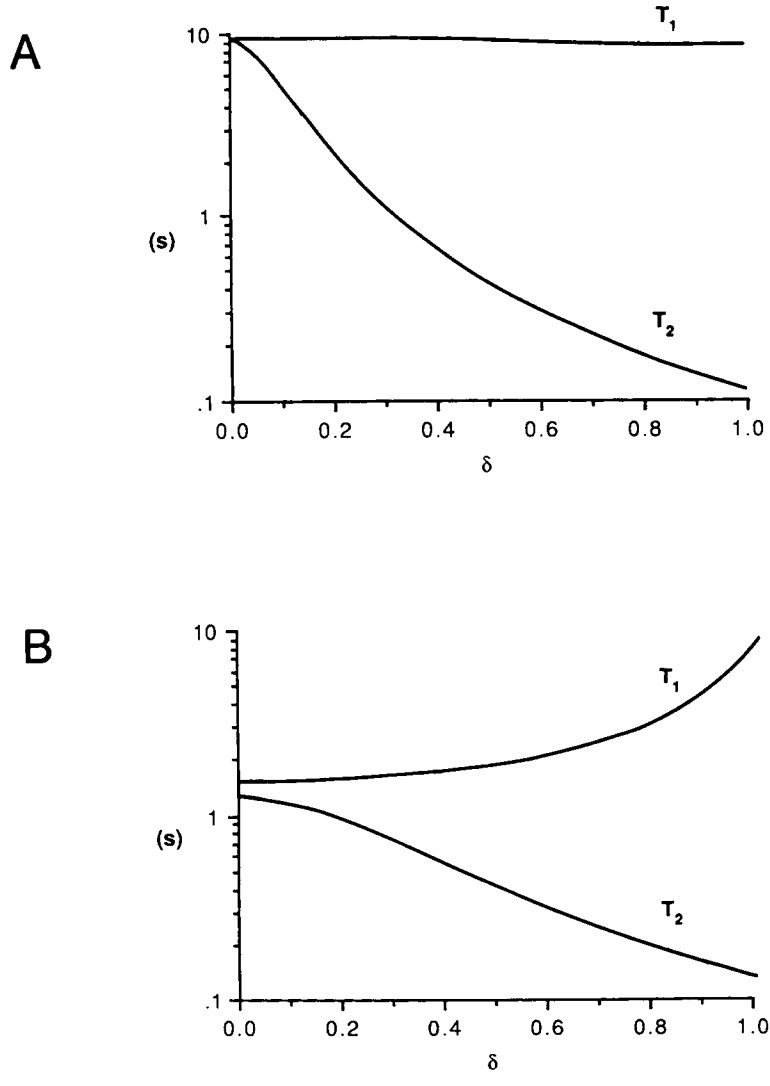

Fig. 2. Calculated spin–lattice and spin–spin relaxation times at 600 MHz for a proton relaxed by two other protons at 0.2 nm, using the order parameter model.[33] Correlation time for overall molecular tumbling is 2.7 ns. δ is the order parameter. (A) τ_e = 0.01 ns; (B) τ_e = 0.1 ns.

lattice and spin–spin relaxation times were calculated for the order parameter model and Woessner's model using an overall tumbling correlation time of 2.7 ns.

Figure 2 shows, as a function of the order parameter δ, the T_1 and T_2 values for a proton relaxed by two other protons, each at 0.2 nm, and with a τ_e of 0.01 or 0.1 ns. It is clear that for a τ_e of 0.01 ns, T_1 contributes little to the definition of δ, while for a τ_e of 0.1 ns, T_1 becomes relatively insensitive for $\delta \leq 0.5$. These values for τ_e are within the range found for AP-A (Table II). The effect of this insensitivity is well demonstrated by considering the results obtained when combining data from different measurements. For the order parameter model, a minimum of five exact relaxation times is required, but

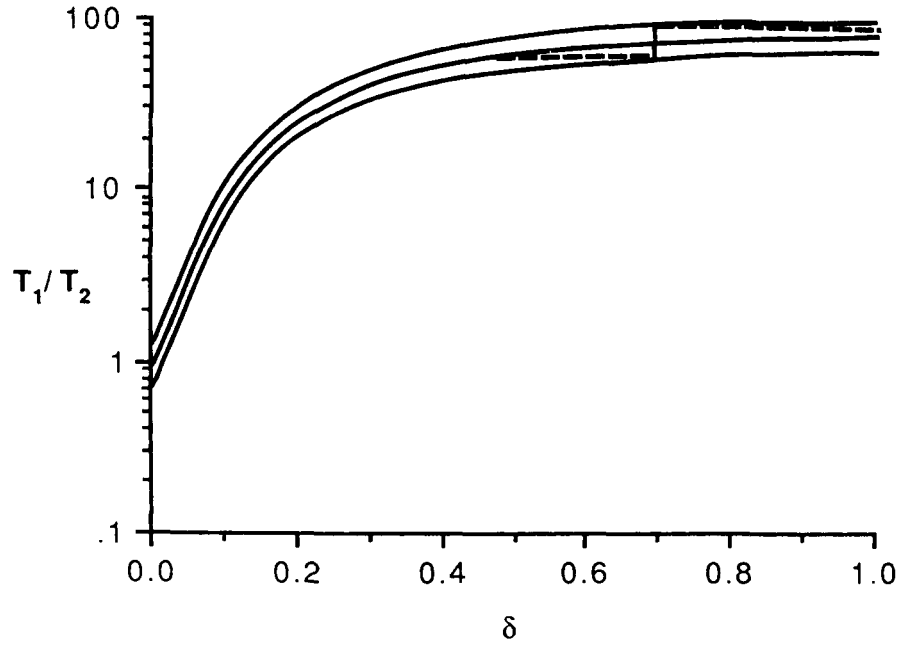

Fig. 3. Calculated T_1/T_2 ratios at 600 MHz using the order parameter model.[33] Correlation time for overall molecular tumbling is 2.7 ns, τ_e = 0.001 ns. Curves corresponding to 10% errors in T_1 and T_2 are also shown.

considering the lack of sensitivity of some of the measurements to physically relevant motions, this may not be adequate. If experimental errors, arbitrarily estimated at 10%, are introduced, uncertainty in fitted parameters becomes worse, but in a manner that depends on the size of the motional parameters. In a simplified case where one knows all the parameters except one, such as the order parameter, the simultaneous equations could be solved at one frequency by using the T_1/T_2 ratio. Figure 3 shows this ratio at 600 MHz with τ_c = 2.7 ns and τ_e = 0.001 ns. Also plotted are the ratios with 10% errors in the T_1 and T_2 measurements. From the shape of the curve, it appears that if δ = 0.7, but the ratio were underestimated, the fitted δ would be incorrect by about 33%. If the ratio were overestimated, the fitted δ would be almost meaningless. This kind of analysis demonstrates that a simple random error in the measurements can lead to an error that is not symmetric about the correct solution and that 10% experimental error may lead to more than a 10% error in the fitted parameters. Furthermore, the uncertainty in δ depends on the size of δ.

For the case of methyl resonances, Fig. 4 shows T_1 and T_2 relaxation times at 600 MHz as a function of τ_{Me} in Woessner's model [Eq. (7)] for the three-site jump model. Again, for the purpose of example, τ_c is set at 2.7 ns. It is evident that T_2 is relatively insensitive to τ_{Me} over this range (particularly for fast internal motions), while T_1 is insensitive for τ_{Me} near 0.1 ns.

These considerations serve to emphasize that not all relaxation measurements made over a range of experimentally accessible frequencies are equally useful in defining motional parameters in a molecule such as AP-A. In

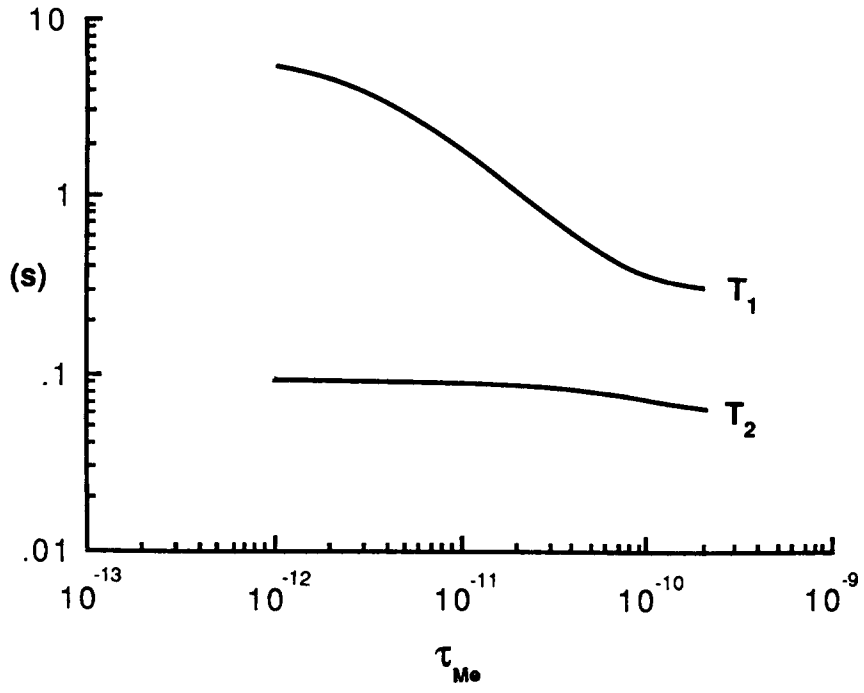

Fig. 4. Calculated spin–lattice and spin–spin relaxation times for a methyl proton at 600 MHz using Woessner's model.[32] Correlation time for overall molecular tumbling is 2.7 ns. τ_{Me} is the correlation time for rotation of the methyl group.

practice, of course, these effects are minimized by fitting all data simultaneously. In the calculations, τ_c, τ_e, and τ_{Me} were set to typical but arbitrary values, whereas they were variable parameters during the actual fitting process. A simple optimizer, as used here, will distribute errors most to those parameters with the least contribution to the penalty function. Thus, the error will be highest for those parameters describing the motions that are least well sampled by the measurements.

Aside from the effect of experimental errors, certain assumptions have been made in our analysis related to the nature of the relaxation processes. The use of Eqs. (4) and (5) is valid if dipolar interactions are the dominant relaxation mechanism. Furthermore, we have simply summed over n interactions and assumed them equivalent, although n was a variable in the fitting process. Similarly, implicit in the use of Eqs. (4) and (5) is the assumption that the dipolar vectors associated with the dominant relaxation pathways have invariant geometry. This is the case for methyl protons, but may be only a reasonable approximation for other sites. The effect of these essential assumptions will be to introduce additional uncertainties in the fitted parameters, but in a manner more difficult to quantify.

Motional Characteristics of AP-A

In light of the above caveats, some conclusions can still be drawn regarding the motions of AP-A in aqueous solution. The poor fits obtained using the

isotropic rotation model implied that overall motion was anisotropic and/or that internal motions were significant. Evidence for both was afforded by the model-free approach of Lipari and Szabo,[33] where good fits to the data were obtained with internal motions having correlation times ranging from 5 to 300 ps, but with correlation times for overall motion ranging from 2.2 to 3.2 ns. The spread of best-fit values for τ_c indicates that overall rotational reorientation was anisotropic. We have avoided any motional models that specify the nature of the internal motions, but given the constrained location of many of the sites, the fast motions probably correspond to small amplitude displacements rather than full rotations. Relaxation measurements over a wider range of spectrometer frequencies would be required to define these motions in physical terms.

For the methyl protons, the important assumption was made that motions of the center of the methyl group with respect to the whole molecule could be ignored. This is almost certainly an oversimplification, since a methyl group will experience rotations of differing rates about differing axes, as well as the relative internal motions of that backbone segment. Nevertheless, the model gave an adequate fit to the data. As for aromatic and aliphatic methine protons, the size and rate of additional motions could be determined only with additional measurements over a greater range of spectrometer frequencies. Within the scope of the data, it appears that Thr 17 and 42 are the least restricted and Thr 21 the most constrained of the methyl groups. This is consistent with NOE data,[5,6] which show few observable interactions for Thr 42 or 17, but show Thr 21 to be close to residues 3, 23, 33, and 47.

It is of interest to compare our data with other studies of polypeptides of similar size. In erabutoxin,[23] the backbone α-protons displayed no detectable anisotropy even though measurements were made at 270 and 500 MHz. If motion had been detectably anisotropic, more measurements would have been necessary to define additional correlation times, but the range of frequencies used should have been adequate to show any deviation from isotropic motion. Richarz et al.[9] used ^{13}C-nmr T_1, NOE, and line-width measurements at 25 and 90 MHz to study bovine pancreatic trypsin inhibitor. Although the α-carbon resonances provided little evidence for librational motions of the backbone, strong evidence for such motions was found in the relaxation behavior of six Ala β-carbons. Using the wobbling in a cone model,[38] these motions were found to have time scales of 1–3 ns. Ribeiro et al.[37] also studied the trypsin inhibitor with ^{13}C-nmr. Using T_1 and NOE measurements at 45 and 90 MHz, they obtained correlation times broadly similar to those presented here. They used a single estimate for τ_c taken from light scattering and found it necessary to use three correlation times ranging from 0.001 to 20 ns to explain the relaxation behavior of the backbone α-carbons. It would be of interest to determine if the fit to their data deteriorated if only two correlation times were used but without recourse to the assumption of a contribution to all sites arising from a common correlation time.

CONCLUSIONS

In general terms, it is worthwhile to judge the use of ^{1}H-nmr relaxation measurements for defining molecular motions. Cursory assessment of the type

of data necessary to distinguish models of the spectral density function and values for associated parameters suggests that $(n + 1)$ measurements are necessary to determine n parameters. Furthermore, the type of measurement should be such as to cover the best sampling of the spectral density function. These statements are, in practice, not strictly true. As we have seen, T_2 measurements may contribute little information under some circumstances since their variation within the range of physically plausible correlation times may be smaller than experimental error. This qualification is also relevant to data from $T_{1\rho}$ measurements that offer a similar sampling of $J(\omega)$ but are even more experimentally demanding. Ideally, one would like to use a wider range of spectrometer frequencies, but practical considerations impose upper limits on this approach. It may, in fact, be more profitable to extend the frequency range by working at lower frequencies, and overcome the loss of resolution by using two-dimensional nmr, as described by Arseniev et al.[39]

Another method for increasing the frequency range sampled would be to include data from more than one type of nucleus. Although ^{1}H and ^{13}C relaxation studies on the same protein may be used to confirm each other, it would be more useful to treat both types of measurement as part of the same data set. In our study, simultaneous regression was performed onto Eqs. (4) and (5), but it would be straightforward to extend the procedure to include expressions for ^{13}C T_1 or NOE measurements substituted with the appropriate spectral density function adapted for the geometry of the proton-carbon vectors. Resolution and sensitivity in the carbon spectrum might also be improved by combining the two-dimensional approach of Arseniev et al.[39] with ^{1}H detection of ^{13}C magnetization via polarization transfer.[40,41] It should be noted that analysis of combined ^{1}H- and ^{13}C-nmr relaxation data would be straightforward only in certain situations such as methyl and methylene groups where motions of the individual proton–proton and proton–carbon internuclear vectors could be related to a common set of motions. In conclusion, it appears that ^{1}H relaxation times alone will be most useful only when motions are simple or where appropriate physical assumptions can be justified. Their role may be seen as just one component of a series of measurements necessary to define complicated macromolecular motions.

We thank Drs. M. Batley and C. M. Fookes for access to the XL-200 and GX-400 spectrometers, respectively. Financial support for this work was provided in part by the Australian Research Grants Scheme.

References

1. Norton, T. R. (1981) *Fed. Proc.* **40**, 21–25.

2. Scriabine, A., Van Arman, C. G., Morgan, G., Morris, A. A., Bennett, C. D. & Bohidar, N. R. (1979) *J. Cardiovasc. Pharmacol.* **1**, 571–583.

3. Smith, C. D., DeLucas, L., Ealick, S. E., Schweitz. H., Lazdunski, M. & Bugg, C. E. (1984) *J. Biol. Chem.* **259**, 8010–8011.

4. Gooley, P. R. & Norton, R. S. (1985) *Eur. J. Biochem.* **153**, 529–539.

5. Gooley, P. R. & Norton, R. S. (1986) *Biochemistry* **25**, 2349–2356.

6. Torda, A. E., Mabbutt, B. C., Van Gunsteren, W. F. & Norton, R. S. (1988) *FEBS Lett.*, in press.

7. Torda, A. E. & Norton, R. S. (1987) *Biochem. Intl.* **15**, 659–666.

8. Wilbur, D. J., Norton, R. S., Clouse, A. O., Addleman, R. & Allerhand, A. (1976) *J. Am. Chem. Soc.* **98**, 8250–8254.

9. Richarz, R., Nagayama, K. & Wüthrich, K. (1980) *Biochemistry* **19**, 5189–5196.
10. Jardetzky, O., Ribeiro, A. A. & King, R. (1980) *Biochem. Biophys. Res. Commun.* **92**, 883–888.
11. Inagaki, F., Miyazawa, T., Tamiya, N. & Williams, R. J. P. (1982) *Eur. J. Biochem.* **123**, 275–282.
12. Sherry, A. D., Keepers, J., James, T. L. & Teherani, J. (1984) *Biochemistry* **23**, 3181–3185.
13. London, R. E. (1980) in *Magnetic Resonance in Biology*, Cohen, J. S., Ed., John Wiley & Son, New York, pp. 1–69.
14. Kalk, A. & Berendsen, H. J. C. (1976) *J. Magn. Reson.* **24**, 343–366.
15. Campbell, I. D. & Freeman, R. (1973) *J. Magn. Reson.* **11**, 143–162.
16. Sykes, B. D., Hull, W. E. & Snyder, G. H. (1978) *Biophys. J.* **21**, 137–146.
17. Cutnell, J. D. & Glasel, J. A. (1976) *J. Am. Chem. Soc.* **98**, 7542–7547.
18. Kay, L. E. & Prestegard, J. H. (1987) *J. Am. Chem. Soc.* **109**, 3829–3835.
19. Jones, C. R., Sikakana, C. T., Hehir, S. P. & Gibbons, W. A. (1978) *Biochem. Biophys. Res. Commun.* **83**, 1380–1387.
20. Niccolai, N., de Leon de Miles, M. P., Hehir, S. P. & Gibbons, W. A. (1978) *J. Am. Chem. Soc.* **100**, 6528–6529.
21. Kuo, M.-C., Drakenberg, T. & Gibbons, W. A. (1980) *J. Am. Chem. Soc.* **102**, 520–524.
22. Olejniczak, E. T., Poulsen, F. M. & Dobson, C. M. (1981) *J. Am. Chem. Soc.* **103**, 6574–6580.
23. Inagaki, F., Boyd, J., Campbell, I. D., Clayden, N. J., Hull, W. E., Tamiya, N. & Williams, R. J. P. (1982) *Eur. J. Biochem.* **121**, 609–616.
24. Schweitz, H., Vincent, J.-P., Barhanin, J., Frelin, C., Linden, G., Hugues, M. & Lazdunski, M. (1981) *Biochemistry* **20**, 5245–5252.
25. Gooley, P. R., Blunt, J. W., Beress, L. & Norton, R. S. (1988) *Biopolymers* **27**, 1143–1157.
26. Carr, H. Y. & Purcell, E. M. (1954) *Phys. Rev.* **94**, 630–639.
27. Meiboom, S. & Gill, D. (1958) *Rev. Sci. Instrum.* **29**, 688–691.
28. Gutowsky, H. S., Vold, R. L. & Wells, E. J. (1965) *J. Chem. Phys.* **43**, 4107–4125.
29. Freeman, R. & Hill, H. D. W. (1975) in *Dynamic Nuclear Magnetic Resonance Spectroscopy*, Jackman, L. M. & Cotton, F. A., Eds., Academic Press, New York, pp. 131–162.
30. Veng-Pedersen, P. (1977) *J. Pharmacokinet. Biopharmaceut.* **9**, 513–531.
31. Ejchart, A., Oleski, P. & Wroblewski, K. (1984) *J. Magn. Reson.* **59**, 446–451.
32. Woessner, D. E. (1962) *J. Chem. Phys.* **36**, 1–4.
33. Lipari, G. & Szabo, A. (1982) *J. Am. Chem. Soc.* **104**, 4546–4559, 4559–4570.
34. Craik, D. J., Kumar, A. & Levy, G. C. (1983) *J. Chem. Inf. Comp. Sci.* **23**, 30–38.
35. Imoto, T., Johnson, L. N., North, A. C. T., Phillips, D. C & Rupley, J. A. (1972) in *The Enzymes*, Vol VII, Boyer, P. D., Ed., Academic Press, New York, pp. 665–868.
36. Squire, P. G., Moser, P. & O'Konski, C. T. (1968) *Biochemistry* **7**, 4261–4272.
37. Ribeiro, A. A., King, R. R., Restivo, C. & Jardetzky, O. (1980) *J. Am. Chem. Soc.* **102**, 4040–4051.
38. Kinosita, K., Jr., Kawato, S. & Ikegami, A. (1977) *Biophys. J.* **20**, 289–305.
39. Arseniev, A. S., Sobol, A. G. & Bystrov, V. F. (1986) *J. Magn. Reson.* **70**, 427–435.
40. Sklenar, V., Torchia, D. & Bax, A. (1987) *J. Magn. Reson.* **73**, 375–379.
41. Kay, L. E., Jue, T. L., Bangerter, B. & Demou, P. C. (1987) *J. Magn. Reson.* **73**, 558–564.

Received March 28, 1988
Accepted June 29, 1988